Regular Article

PHYSICAL CHEMISTRY RESEARCH
Published by the
Iranian Chemical Society
www.physchemres.org
info@physchemres.org

Phys. Chem. Res., Vol. 12, No. 2, 333-348, June 2024
DOI: 10.22036/pcr.2023.377616.2331

Computational Investigation of Polo-like Kinase 1 (plk1): Inhibitive Potential of Benzimidazole-Carbonamide Derivatives for Cancer Treatment

N. Ipinloju, T.A. Balogun, A. Ibrahim, M.A. Adeyemo, T.O. Esan, A.V. Emmanuel, K.A. Bello, G.D. Omiyeniyi and O.E. Oyeneyin

[a]*Theoretical and Computational Chemistry Unit, Department of Chemical Sciences, Adekunle Ajasin University, Akungba-Akoko, Ondo State, Nigeria*

[b]*Department of Biochemistry, Adekunle Ajasin University, Akungba-Akoko, Nigeria*

[c]*Department of Biochemistry and Molecular Biology, Usmanu Danfodiyo University, Sokoto, Sokoto State, Nigeria*

[d]*Department of Chemistry, Federal University of Biochemistry Technology, Akure, Nigeria*

[e]*Department of Chemical Sciences, Bamidele Olumilua University of Education Science and Technology, Ikere-Ekiti, Ekiti State, Nigeria*

(Received 1 May 2023, Accepted 19 August 2023)

Cancer is the second most lethal disease worldwide after cardiovascular disease. Discovering and developing new drugs and repurposing existing drugs to curb this disease have gathered interest from researchers globally. In this work, computer-aided approaches *via* density functional theory (DFT), molecular docking, and pharmacokinetics were adopted for the evaluation of anti-breast cancer activity of 2-({4-[(1H-Benzimidazol-2-yl)sulfanyl]phenyl}methylidene)hydrazine-1-carbothioamide and its modified derivatives. In the result, the BMHCd showed the lowest bang gap energy, indicating the most reactive among the compounds. Also, molecular docking showed that all the compounds have stable interactions and higher binding energy, with BMHCf showing the highest (-8.469 kcal mol^{-1}). Furthermore, all the compounds satisfy the Lipinski rule of five and are, therefore, good therapeutic candidates for the treatment of human cancer.

Keywords: Benzimidazole-Carbonamide derivatives, Breast cancer, Density functional theory, Molecular docking

INTRODUCTION

Cancer, also known as a malignant tumor, is a heterogeneous tumor that affects all parts of the body. It is a type of disease in which a group of cells exhibits uncontrollable and rapid growth. According to World Health Organization, cancer is said to be the leading cause of death globally after cardiovascular disease [1] with nearly 10 million deaths recorded in 2020 due to cancer-related disease (WHO, 2021) [1]. One of the most common cancer treatment methods is chemotherapy (the use of drugs). However, most of these drugs have some adverse effects and high multidrug resistance has been reported in some [2-3]. Therefore, it is imperative to design more effective and safer anti-cancer drugs. MCF-7 cell line has been an effective cell line for breast cancer investigation worldwide. The MCF-7 cell line is important in studying the estrogen receptor (*in vivo* and *in vitro*).

Polo-like kinase 1 (PLK1) plays a crucial part in modulating the G2-M phase of the cell cycle [4], which includes the controlling of centrosome maturation and spindle assembly, the deactivation of anaphase-promoting complex/cyclosome (APC/C) inhibitors, the elimination of cohesins from chromosome arms, and the controlling of mitotic exit and cytokinesis [5]. PLK1 is an oncogene that is highly expressed in a variety of cancers, including breast cancer [6]. Small molecule PLK1 blockers lead to a reduction

*Corresponding authors. E-mail: Nureniipinloju@gmail.com; oluwatoba.oyeneyin@aaua.edu.ng, emmanueltoba90@gmail.com

in cancer cell development and a rise in apoptosis as a result of the inhibition of PLK1 inducing mitotic arrest of cancer cells [7].

Heterocyclic compounds have been reported useful in this regard [8-20]. Benzimidazole heterocyclic scaffold is an overwhelming pharmacophore in pharmaceutical and medicinal chemistry, it can be termed the "Master key" due to its great pharmacological potential [11]. It is an important pharmacological active molecule that serves as one of the top ten most used nitrogen-containing heterocycles among the US Food and Drug Administration (FDA) approved drugs [12]. Benzimidazole has several biological activities such as anti-cancer [13], antimicrobial [14], antihelmintic [15], and anti-inflammatory [16]. The therapeutic potential of benzimidazole has drawn the attention of several researchers to design and synthesized more potent derivatives with high pharmacological activities. Benzimidazole has shown several anticancer potentials with various mechanisms to inhibit tumor progression including anti-angiogenesis, disruption of microtubule polymerization, induction of apoptosis, and cell cycle (G2/M) arrest [17]. Also, Thiosemicarbazones are the backbones of many molecules with diverse biological activities like antimalarial [18], anticancer [19], anti-inflammatories [20], anti-HIV [21], and anticonvulsant [22]. Computer-aided drug design is used to predict and design novel molecules with potential therapeutic activities [23-24] with great success. It is a rapid, cheap, and fast method used in predicting and designing novel, highly potent drugs [25]. Density Functional Theory (DFT) is a quantum chemical method employed to predict molecules' structural parameters [26-28]. Molecular docking probes into the right pose of a small molecule inside the target protein (receptor) [29-30]. It identifies the binding sites and bioactivities of a small molecule in the target site [32-33].

2-({4-[(1H-Benzimidazol-2-yl)sulfanyl]phenyl} methylidene)hydrazine-1-carbothioamide (BMHCa) has been synthesized and characterized by (Ubeid *et al*., 2021) [34]. The synthesis procedure is shown in Fig. 1. In this study, we employed DFT and molecular docking studies to investigate the anticancer activity of BMHCa and its derivatives for the first time. The derivatives are from the inclusion of CH_3 (BMHCb), NH_2 (BMHCc), $NHCOCH_3$ (BMHCd), OCH_3 (BMHCe), and OH (BMHCf) into the phenyl ring in benzimidazole moiety (Fig. 2). These derivatives have been proved to enhance the reactivity and bioactivity of a molecule as highlighted by previous work [35].

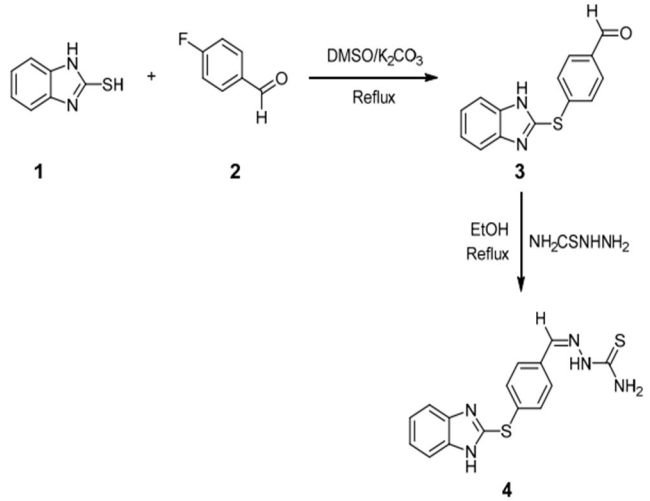

Fig. 1. The synthesis procedure of BHMCa [34].

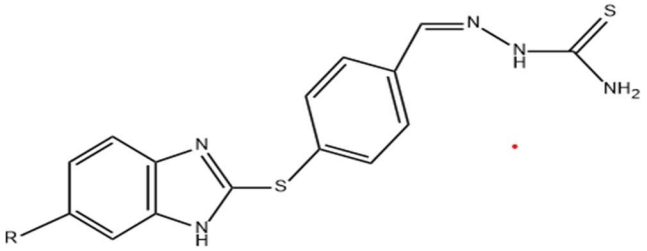

(1) R = H (BHMCa),
(2) R = CH_3 (BHMCb),
(3) R = NH_2 (BMHCc),
(4) R = $NHCOCH_3$ (BMHCd),
(5) R = OCH_3 (BMHCe),
(6) R = OH (BMHCf)

Fig. 2. Structures of BMHC and its derivatives.

METHODOLOGY

DFT Calculations

DFT is used to investigate the stability and chemical reactivity of a molecule [36]. The DFT quantum analysis for the ground state electronic properties and reactivity indices of the compounds was performed using SPARTAN 14

software [37]. The structures of the compounds were modelled using Spartan 14. The most stable conformers of each compound were searched using molecular mechanics Force Field (MMFF) before geometric optimization at the DFT/B3LYP [38] and 6-31G* basis set [39]. The calculated molecular properties are the energies of the frontier molecular orbitals (E_{HOMO} and E_{LUMO}). A higher value of E_{HOMO} signifies a reasonable potential of a molecule to donate electronic density readily to nearby atoms and lower E_{LUMO} indicates the ability to accept electronic density [40]. The reactivity of a molecule is enhanced with an increase in E_{HOMO} energy and a decrease in E_{LUMO} energy. The band gap energy (ΔE) can be defined as the difference between the energy of LUMO and HOMO (Eq. (1)) and is another vital parameter to predict the stability and reactivity of a molecule. A larger value of the energy band gap implies high chemical stability and low reactivity while a lower value of band gap energy signifies high reactivity and low chemical inertness [41-42].

$$\Delta E = E_{LUMO} - E_{HOMO} \quad (1)$$

Furthermore, some other properties used to describe the reactivity of a molecule (reactivity descriptors) were also calculated. Ionization energy (I) and electron affinity (A) according to a theorem proposed by Koopmans [43] are related to the energy of HOMO and LUMO (Eq. (2) and Eq. (3)).

$$I = -E_{HOMO} \quad (2)$$

$$A = -E_{LUMO} \quad (3)$$

Electronegativity (χ), and chemical potential (μ) according to Parr and Pearson [44], can be expressed in the function of ionization energy and electron affinity (Eq. (4)). The chemical hardness (η) and softness (S) can be expressed using Parr and Pearson theorem [44] in Eqs. (5) and (6) respectively.

$$\chi = -\mu = \frac{I+A}{2} \quad (4)$$

$$\eta = \frac{I-A}{2} \quad (5)$$

$$S = \frac{1}{\eta} \quad (6)$$

Molecular Docking Study

Protein preparation and Receptor grid generation. The crystal structure of the target receptor PLK (3FC2) with a 2.45 Å resolution factor was retrieved from the PDB database. The protein structure was prepared by the addition of the hydrogen atoms, setting of bond order, removal of the water molecule, replacement of missing atoms, and addition of side chain implementing the "Protein Preparation module" in the Schrodinger suite 2018 software [45]. OPLS3 was applied to save energy. The grid box was obtained using receptor grid generation. The grid was created by selecting the co-crystallized ligand which provides an insight into the active site of the receptor through the coordinate ((X: 48.26, Y: -7.45, and Z: 9.56) [46-47].

Ligand Preparation

Employing Spartan 14.4 software tool, the 3D structure of Benzimidazole-Carbonamide and five of its derivatives were modelled by varying its functional group. The standard ligand Volasertib was downloaded from the PubChem website. The ligands were prepared using the LigPrep tool of Schrodinger suite 2018, which included the generation of tautomers and ionization states at neutral pH. Hydrogen atoms were added and charged groups were neutralized using Epik [45-46]

Molecular Docking

The extra precision method was used to dock the compounds at the active site of the 3FC2 with the aid of the generated grid box parameters (X: 48.26, Y: -7.45, and Z: 9.56 respectively) [48]. Additionally, the co-crystallized ligand retrieved from the protein was re-docked at the active site of the protein and its RMSD value was observed at 1.50 Å which supports the validation and reproducibility of the docking method [49-53].

Drug-likeness Properties

The studied compounds' drug-likeness parameters were analyzed using the SwissADME web server (http://www.swissadme.ch/).

In silico Pharmacokinetics Prediction

The absorption, distribution, metabolism, excretion, and toxicity (ADMET) properties were predicted using the admetSAR online server (admetSAR (ecust.edu.cn) [53].

RESULTS AND DISCUSSIONS

Global Reactivity Descriptors

The descriptors computed for the Benzimidazole-carbonamide derivatives are shown in Table 1. The HOMO energies of the studied molecules are in order: BHMCc (-5.40 eV) > BHMCd (-5.45 eV) > BHMCe (-5.56 eV) > BHMCb (-5.59 eV) > BHMCf (-5.60 eV) BHMCa (-5.61 eV). BHMCc has the highest HOMO orbital energy value (E_{HOMO} = -5.40 eV), indicating that there is more ability of electron density distribution of BHMCc than other derivatives, hence BHMCc should donate electrons more readily to a nearby molecule. The LUMO energy shows the ability of a molecule to accept electrons from neighboring atoms. The lower the LUMO energy, the higher the ability to accept electrons [54]. BHMCa (-1.80 eV) had the lowest LUMO energy value indicating a high tendency to accept electrons. The HOMO structure of molecules 1, 2, and 5 shows HOMO distribution over the hydrazinecarbothioamide moiety (Table 2). In BHMCc and BHMCd, the HOMO structure shows the distribution of HOMO over the benzimidazole ring. This is because of the attachment of a more electron-donating group (NH_2 and $NHCONH_3$) to benzene in the benzimidazole ring. This enhances the electron-releasing ability of the compounds. All the molecules show a distribution of LUMO over thiobenzylidenes-hydrazinecarbothioamide (Table 2).

The tendency of a molecule to be more reactive can be observed using the HOMO-LUMO energy gap (ΔE) since this value is related directly to the reactivity of a molecule [54]. The lower the ΔE, the higher the reactivity. ΔE values calculated for all the derivatives are shown in Table 1, The values are in order: BHMCd < BHMCc < BHMCa < BHMCb < BHMCf < BHMCe. BHMCd showed the lowest energy gap hence, the most reactive among the molecules. Chemical hardness (η) measures the resistance toward electron cloud deformation of a system [55]. Hard molecules usually have high stability while chemical softness (S) measures the ability of a system to be subject to the distribution of electron density thereby increasing the reactivity of a molecule. BHMCd shows the highest chemical softness (0.50 eV^{-1}) which may contribute to the higher reactivity among the studied compounds. The chemical hardness varies in the order BHMCe > BHMCf > BHMCb > BHMCa > BHMCc > BHMCd. BHMCd also has the lowest chemical hardness.

Molecular Electrostatic Potential (MEP) Map and Analysis

The MEP map provides insight into the site of a molecule with excess electrons and the site with electron deficiency. Negative electrostatic potential shows specific sites in a molecule for an electrophilic attack. The electrostatic potential can be represented by utilizing color to show the value of the potential. The red color indicates the site of the molecule with negative electrostatic potential while the blue color indicates the site with positive electrostatic potential. It follows the order: blue > green > orange > red. All maps are shown in Figs. 3, 4, 5, 6, 7 and 8. The sites liable to nucleophilic attack are mainly hydrogen atoms in all the

Table 1. Quantum Chemical Parameters Calculated

Name	E_{HOMO} (eV)	E_{LUMO} (eV)	ΔE (eV)	I (eV)	A (eV)	η (eV)	δ (eV^{-1})	χ (eV)
BHMCa	-5.61	-1.80	3.81	5.61	1.80	1.91	0.52	3.71
BHMCb	-5.59	-1.68	3.91	5.59	1.68	1.95	0.51	3.64
BHMCc	-5.40	-1.63	3.77	5.40	1.63	1.89	0.53	3.52
BHMCd	-5.45	-1.77	3.68	5.45	1.77	1.84	0.54	3.61
BHMCe	-5.56	-1.63	3.93	5.56	1.63	1.97	0.50	3.60
BHMCf	-5.60	-1.68	3.92	5.60	1.68	1.96	0.51	3.64

Table 2. Optimized Structure, HOMO Structure, and LUMO Structure

Optimized structure	HOMO map	LUMO map
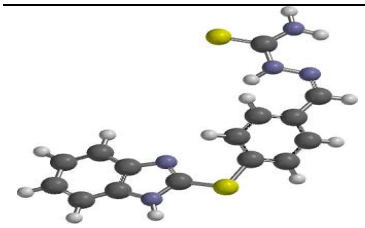 BHMCa	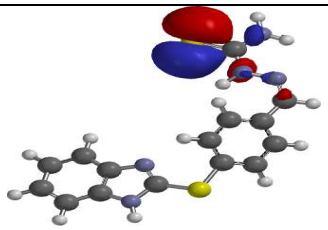	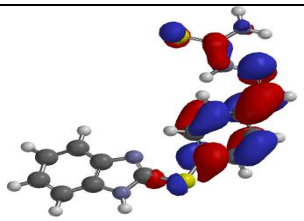
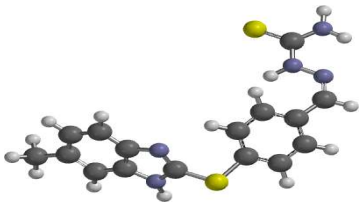 BHMCb	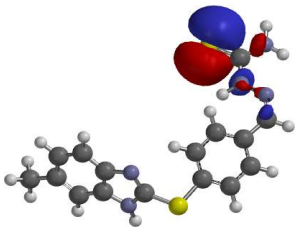	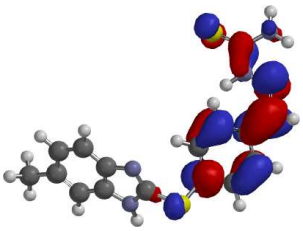
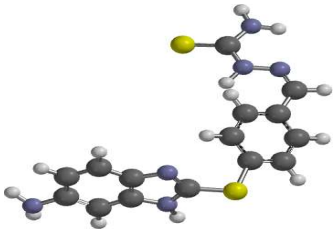 BHMCc	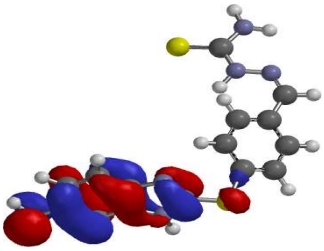	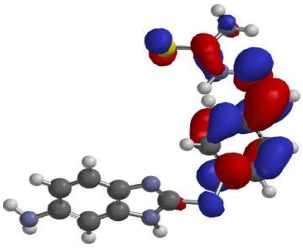
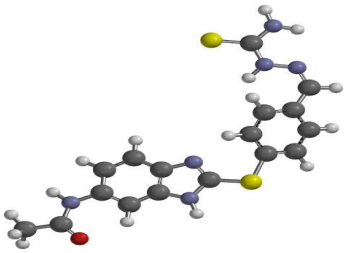 BHMCd	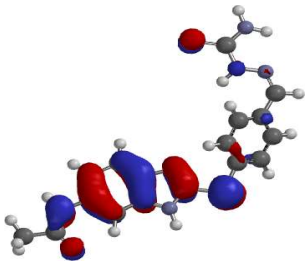	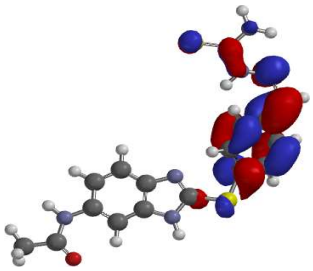
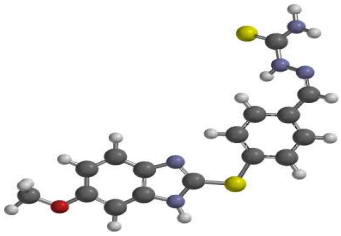 BHMCe	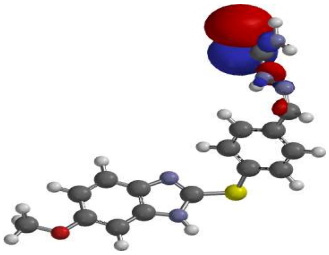	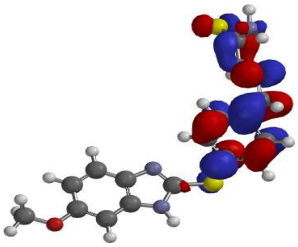
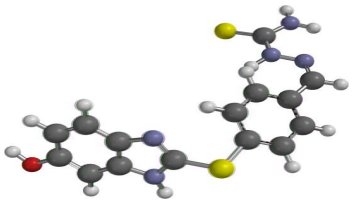 BHMCf	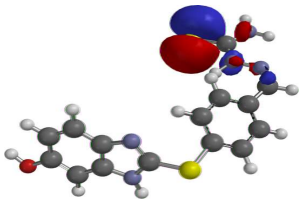	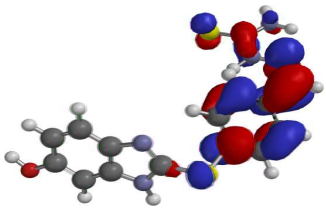

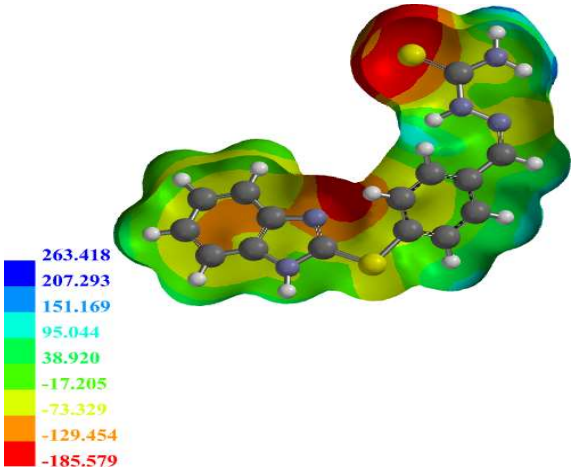

Fig. 3. MEP map BHMCa.

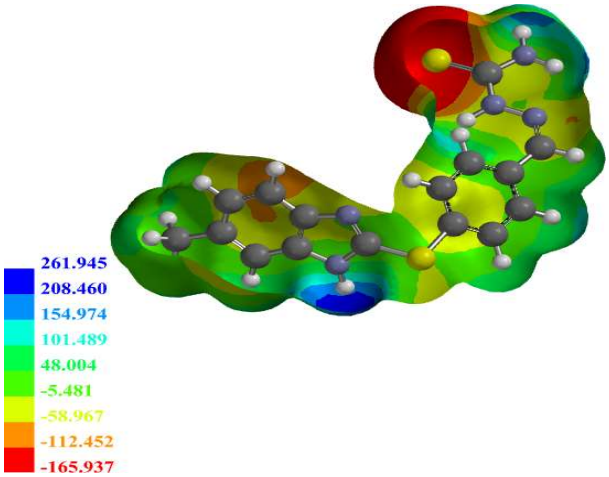

Fig. 4. MEP map of BHMCb.

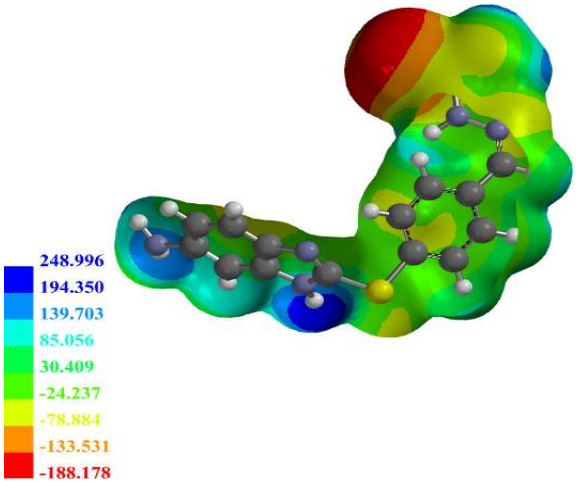

Fig. 5. MEP map of BHMCc.

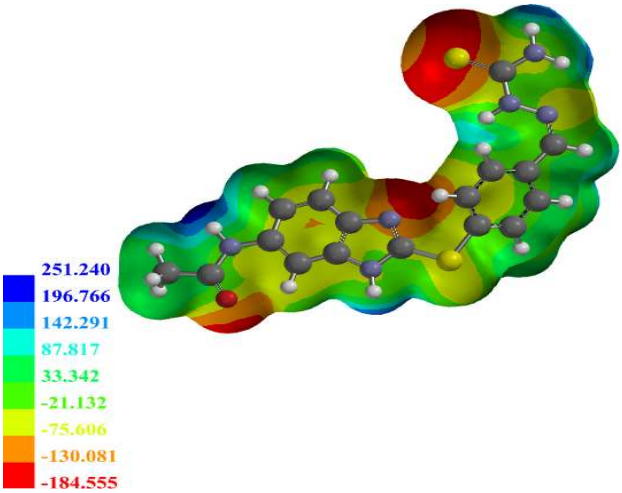

Fig. 6. MEP map of BHMCd.

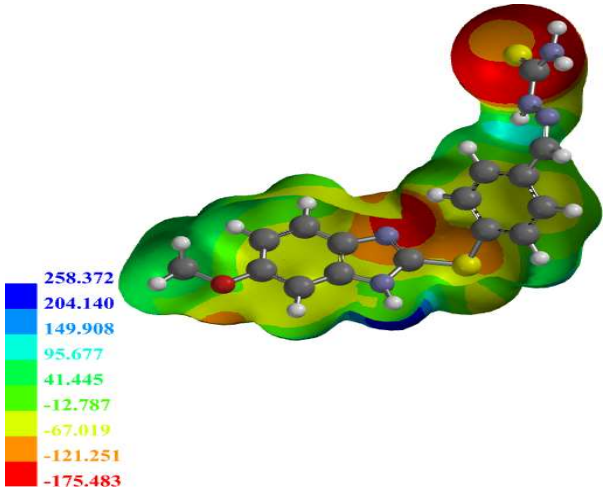

Fig. 7. MEP map of BHMCe.

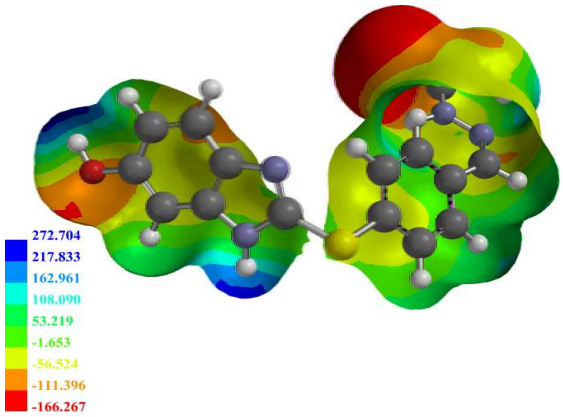

Fig. 8. MEP map of BHMCf.

rings. The heteroatoms (nitrogen, oxygen, and sulphur) in the rings of all studied compounds show negative electrostatic potential indicating the site is susceptible to electrophilic attack.

Thermochemical Analysis

Optimization of molecular interaction between the lead compound and the target receptor is a key part of drug design and discovery. Thermodynamic properties are important properties for the determination of the spontaneity of chemical reactions and stability of chemical reactions. Gibb's free energy is an important thermodynamic parameter employed in describing the interaction between the ligand and the target receptor. It explains the chance of biomolecular events happening. The ligand-receptor binding interaction will not occur spontaneously if the free energy is positive. Negative free energy indicates that the interaction will be spontaneous and the higher the negative value, the more the spontaneity of the interaction [56]. Hence, the extent to which the ligands interact with 3FC2 is shown by the value of negative free energy while the binding enthalpy shows the energy change occurring during binding. Table 3 shows the enthalpy change and Gibb's free energies of all the molecules. The negative values of Gibb's free energy displayed by all molecules infer spontaneous binding with the receptor.

Molecular Docking

Computer-aided drug design techniques are used for the design of small molecules with potential therapeutic activities. Molecular docking is often employed in structure-based-drug-design (SBDD) because of its potential to predict the conformation of the ligand within the pocket of the receptor and the prediction of ligand-receptor complex structure [57-58].

Human Serine/Threonin-Protein Kinase Receptor, (PDB ID; 3FC2), a crucial protein for mitosis, promotes mitotic entry by phosphorylating CDK1 and cyclin B1 and also causes mitotic exit by activating the cell cycle's Anaphase Promoting Complex (APC) [59]. By bypassing the G2M DNA damage and spindle checkpoints, overexpression of this protein (PLK1) encourages chromosomal diversity and aneuploidy [59]. Numerous malignancies have elevated PLK1 expression, and both in vitro and in vivo tumor growth can be inhibited by pharmacological inhibitors or shRNA [59-60]. All the compounds including the standard were docked at the target receptor's active site. In a previous study, benzimidazole-carbonamide derivatives were tested for their inhibitory properties toward the MCF-7 cell using computational chemistry approaches [61]. Among the studied compounds, the lead compound showed excellent results with binding affinity of -9.350 kcal mol^{-1}. Also, Oyeneyin *et al.* [24] investigated the anti-proliferative potential of heterocyclic amino-chalcone derivatives against MCF-7 breast cancer cell lines *via* computational chemistry methods, it was discovered that the tested compounds displayed good binding interaction with the target receptor. Furthermore, Tahlan *et al.* [62] investigated the anticancer potential of heterocyclic benzimidazole scaffolds against MCF-7 cell line using in-silico and *in-vivo* methods. The results showed good to moderate anticancer activity against the target cancer cell line.

Table 3. Thermochemical Properties of the Compounds

Compounds	Molecular weight (amu)	Electronic energy (au)	Enthalpy (au)	Gibb's free energy (Hartree)
BHMCa	327.44	-1649.55	-1649.27	-1649.33
BHMCb	341.46	-1688.87	-1688.56	-1688.62
BHMCc	342.94	-1704.90	-1704.60	-1704.66
BHMCd	384.49	-1857.32	-1857.15	-1857.20
BHMCe	357.46	-1764.07	-1763.76	-1763.81
BHMCf	343.44	-1724.76	-1724.48	-1724.54

The method provides the binding affinity of the ligands with the target receptor, and the interaction of the ligand with the target receptor, MM-GBSA as shown in Table 4. The results revealed that all the studied compounds displayed high binding affinity for MCF cell in the treatment of breast cancer. The more negative the binding energy, the better the ligand. The binding energy are in order: BHMCf (-8.469 kcal mol^{-1}) > BHMCb (-8.208 kcal mol^{-1}) > BHMCd (-8.142 kcal mol^{-1}) > BHMCe (-8.059 kcal mol^{-1}) > BHMCa (-6.799 kcal mol^{-1}). BHMCf, the best compound, binds firmly within the pocket of the MCF cell while forming hydrogen bond interaction with ASP194, LYS82, CYS133, ARG136, LEU59, and pi-pi interaction with PHE183 amino acid. Similar interactions occur for all other compounds. This implies that all the compounds are capable of inhibiting the target receptor and also, all the compounds have better binding energy and interaction than the positive control, Volasertib (-6.598 kcal mol^{-1}). All interactions are in Figs. 9-15.

The ΔGbind for PLK-ligand complexes was computed using the MM-GBSA [63]. Based on the MM-GBSA results, BHMCa, BHMCb, BHMCc, BHMCd, BHMCe, and BHMCf, demonstrated binding energy of -68.24, -87.09, -76.46, -90.42, -79.77 and -79.40 kcal mol^{-1} respectively. The other molecules bind better than BHMCa (-68.24) kcal mol^{-1}), but all the studied compounds are better than the standard drug, volasertib (-65.97).

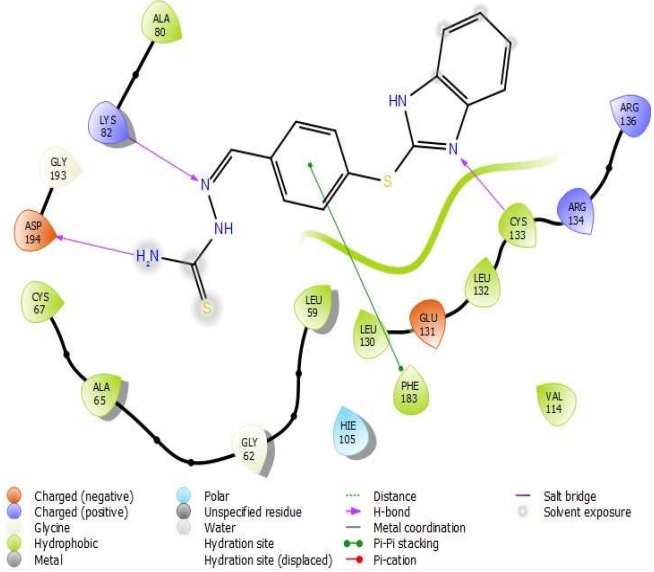

Fig. 9. BHMCa with 3FC2.

Table 4. The Binding Affinity, MM-GBSA, H-bond and Hydrophobic Interaction of the Ligands

Compound	Binding energy (Kcal mol^{-1})	MM-GBSA (Kcal mol^{-1})	Residue involve in the interaction	Type of interaction
BHMCa	-6.799	-68.24	ASP194, LYS82, CYS133, PHE183	Hydrogen bond and pi-pi stacking
BHMCb	-8.208	-87.09	ASP194, LYS82, CYS133, PHE183	Hydrogen bond and pi-pi stacking
BHMCc	-7.834	-76.46	ASP194, LYS82, CYS133, PHE183	Hydrogen bond and pi-pi stacking
BHMCd	-8.142	-90.42	LYS82, ARG134, LEU59, CYS133	Hydrogen bond and pi-pi stacking
BHMCe	-8.059	-79.77	ASP194, LYS82, CYS133, ARG136, PHE183	Hydrogen bond and pi-pi stacking
BHMCf	-8.469	-79.47	ASP194, LYS82, CYS133, ARG136, LEU59, PHE183	Hydrogen bond and pi-pi stacking
Volasertib	-6.598	-65.97	ARG 57, ARG 134	Hydrogen bond

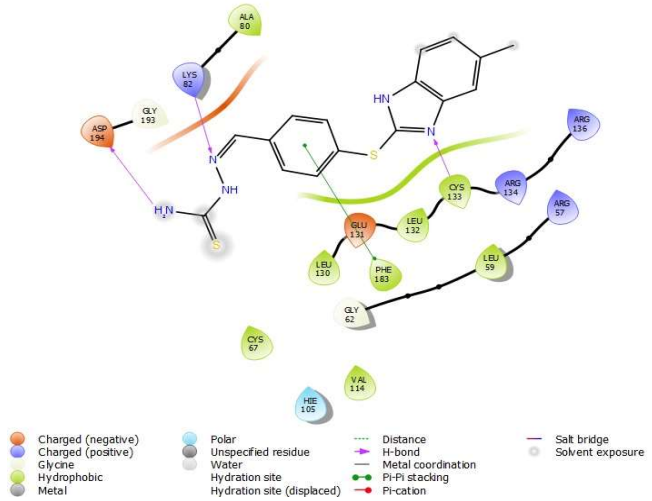

Fig. 10. BHMCb with 3FC2.

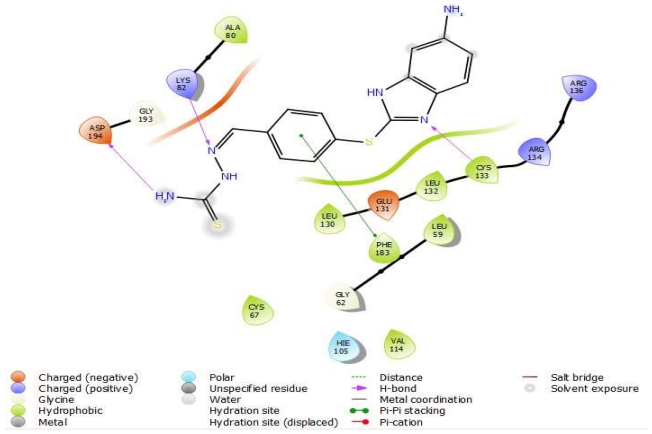

Fig. 11. BHMCc with 3FC2.

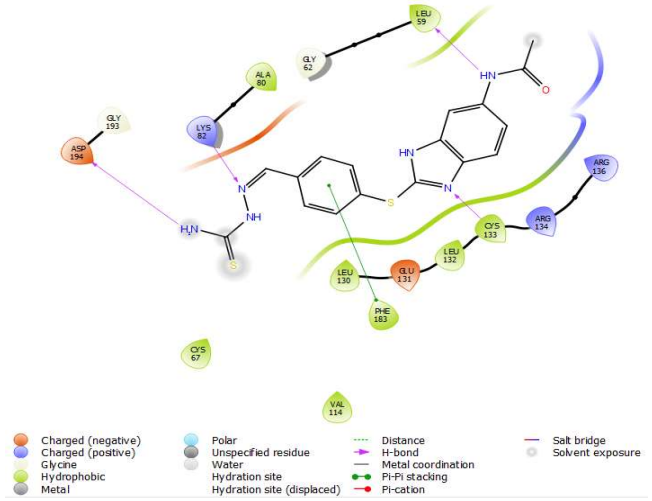

Fig. 12. BHMCd with 3FC2.

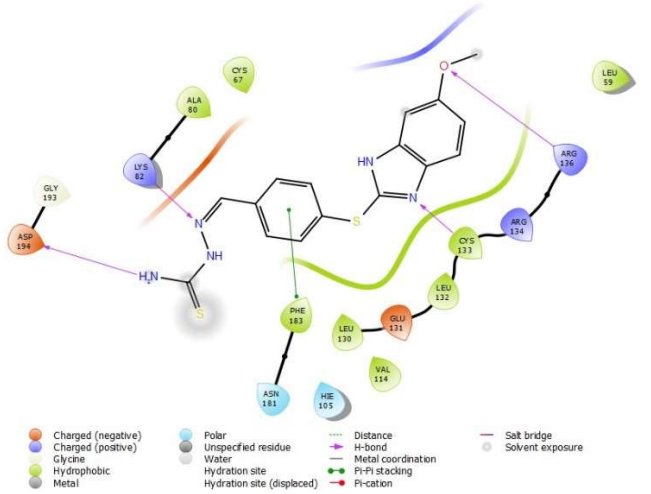

Fig. 13. BHMCe with 3FC2.

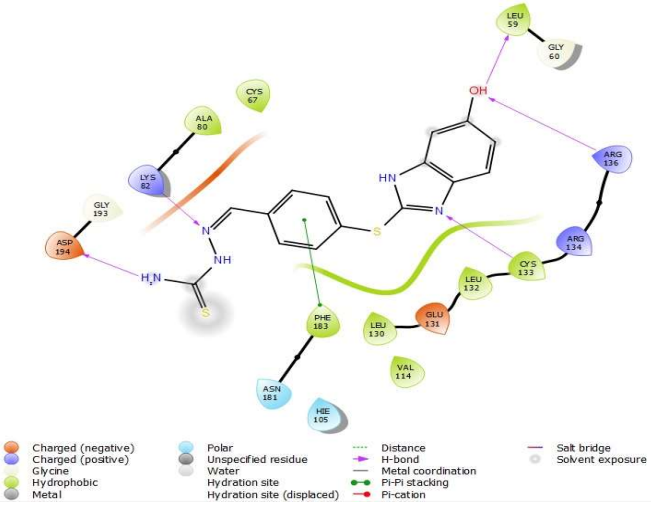

Fig. 14. BHMCf with 3FC2.

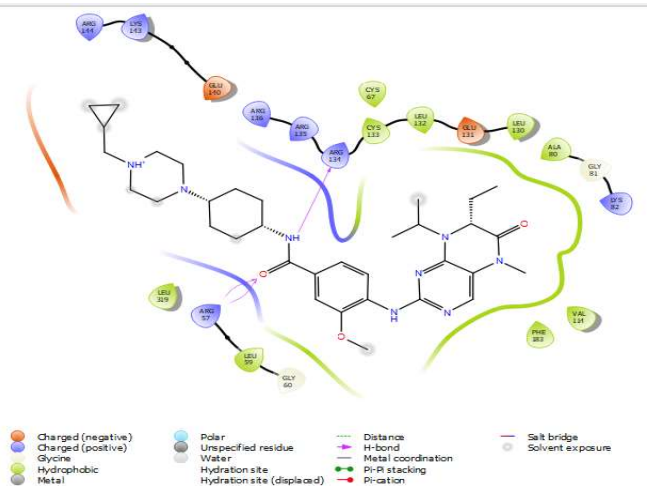

Fig. 15. Volasertib with 3FC2.

Drug-likeness Prediction

The drug-likeness of the studied compounds was examined using the swissADME web server. Lipinski's rule of five is used to predict and evaluate the drug-likeness properties of a bioactive molecule. It determines the potential of a drug to be orally bioactive. According to the rule, an orally bioactive compound should have a hydrogen-bond donor, HBD ≤ 5, hydrogen-bond acceptor, HBA ≤ 10, molecular mass ≤ 500 Da, and octanol-water partition coefficient ≤ 5. Violation of more than one of these is not good. Table 5 shows the lipinkis's properties computed for all the compounds. All the studied compounds conform to these rules which make them promising drugs for cancer treatment. BHMCa has a molecular weight of 327.44 amu, HBD of 3, HBA of 2, and iLOGP of 2.31 which all satisfies Lipinski's rule, BHMCb showed a molecular weight of 341.46 amu, HBD of 3, HBA of 2 and iLOGP of 2.47; it conforms to all the rule.

Furthermore, BHMCc showed MW of 342.45 amu, HBD of 3, HBA of 2, and iLOGP of 1.75; it satisfies all the rules and this also makes it a potential therapeutic molecule for cancer treatment. BHMCd with a molecular weight of 384.48 amu, HBD of 4, HBA of 3, and iLOGP of 2.22 also showed no violation. BHMCe showed a molecular weight of 357.46 amu, HBD of 3, HBA of 3, and iLOGP of 2.44; which also conforms to the rule. Also, BHMCe displayed molecular weight of 343.44 amu, HBD of 3, HBA of 3, and iLOGP of 2.44.

Pharmacokinetics Prediction

The pharmacokinetics prediction of the hit compounds was carried out using admetSAR to estimate how the compounds are absorbed, distributed, metabolized, and eliminated, as well as their potential toxicity in the living system. Table 6 represents the pharmacokinetics result of the compounds as retrieved from the admetSAR server. From the result, BHMCd and BHMCf demonstrated low absorption in the intestine while BHMCa, BHMCb, BHMCc, and BHMCe displayed high intestinal absorption *via* the Caco-2 Permeability, the high intestinal absorption rate may be attributed to their molecular size. All the screened compounds had a positive blood-brain barrier permeation while none of the compounds (BHMCa-BHMCf) were substrates and/or inhibitors of permeability P-glycoprotein (P-GB). The plasma binding protein represents a marker for measuring drug binding to proteins in the blood [64]. A drug's efficaciousness is largely defined by its binding rate. A decrease in plasma protein binding rate indicates better efficiency and ease of diffusion [65]. All the compounds demonstrated a high plasma binding protein which may affect their transport to the site of action where they exert their therapeutic potential. Only compound BHMCc was found primarily in the lysosome while others were in the mitochondria.

Drug metabolism is a significant property because it accounts for nearly 50% of drug excretion *via* Cytochrome P450 enzymes [66]. The therapeutic effects of a drug are highly dependent on metabolism [67]. The most extensively studied CYP450 enzymes, CYP1A2, CYP2C9, CYP2C19, CYP2D6, and CYP3A4/5, metabolize approximately 90% of all drug molecules [68-69]. Table 6 shows that all of the compounds are inhibitors of CYP1A2, with only BHMCa not an inhibitor of CYP2C19. BHMCa and BHMCb was not an inhibitor of CYP2C9. None of the compounds was a substrate

Table 5. Drug-likeness Prediction Properties of the Screened Compounds

Compounds	Molecular weight	H-bond acceptors	H-bond donors	TPSA	iLOGP	Lipinski violations
BHMCa	327.43	2	3	136.48	2.31	0
BHMCb	341.45	2	3	136.48	2.47	0
BHMCc	342.44	2	4	162.5	1.75	0
BHMCd	384.48	3	4	165.58	2.22	0
BHMCe	357.45	3	3	145.71	2.44	0
BHMCf	343.43	3	4	156.71	1.92	0

Table 6. Pharmacokinetics Parameters of the Compounds

Parameters/Compounds	BHMCa	BHMCb	BHMCc	BHMCd	BHMCe	BHMCf
Ames mutagenesis	+	+	+	+	+	+
Acute oral toxicity (c)	III	III	III	III	III	III
Blood-brain barrier	+	+	+	+	+	+
Caco-2	+	+	+	-	+	-
Carcinogenicity	-	-	-	-	-	-
CYP1A2 inhibition	+	+	+	+	+	+
CYP2C19 inhibition	-	+	+	+	+	+
CYP2C9 inhibition	-	-	+	+	+	+
CYP2C9 substrate	-	-	-	-	-	-
CYP2D6 inhibition	-	-	-	-	-	-
CYP2D6 substrate	-	-	-	-	-	-
CYP3A4 inhibition	+	+	+	+	+	+
CYP3A4 substrate	-	+	-	+	+	+
CYP inhibitory promiscuity	+	+	+	+	+	+
Estrogen receptor binding	+	+	+	+	+	+
Hepatotoxicity	+	+	+	+	+	+
Human ether-a-go-go-related gene inhibition	-	+	-	+	+	-
Human intestinal absorption	+	+	+	+	+	+
Human oral bioavailability	+	+	-	-	+	-
Mitochondrial toxicity	+	+	+	+	+	+
Nephrotoxicity	-	-	-	-	-	-
Acute oral toxicity	3.550884	3.226225	3.136393	2.878478	3.311134	2.935427
P-glycoprotein inhibitior	-	-	-	-	-	-
P-glycoprotein substrate	-	-	-	+	-	-
Plasma protein binding	0.638416	0.709361	0.663032	0.484754	0.812094	0.6499
Reproductive toxicity	+	+	+	+	-	-
Respiratory toxicity	+	+	+	+	+	+
skin sensitization	-	-	-	-	-	-
Subcellular localization	Mitochondria	Mitochondria	Lysosomes	Mitochondria	Mitochondria	Mitochondria
UGT catalyzed	-	-	-	-	-	+
Water solubility	-3.29463	-3.2238	-3.24863	-3.48643	-3.50073	-3.53397

of CYP2C9 and CYP2D6 and at the same time, none was an inhibitor of CYP2D6. Compound BHMCa-BHMCf were not inhibitors of CYP3A4 while all the compounds except BHMCa and BMHCc were not a substrate of CYP3A4.

Because of toxicity, many drug candidates fail before reaching clinical trials [70]. The toxicity of the compounds was determined by testing them for carcinogenicity, hepatotoxicity, human ether-a-go-go inhibition, and Ames mutagenesis. As seen in Table 6 all the compounds (BHMCa-BHMCf) were found to be toxic in Ames' test, and none was

found to be carcinogenic. Except for BHMCa, BHMCc, and BHMCf, all of the compounds were shown to inhibit human ether-a-go-go. All the compounds were shown to have no toxic effect on the kidney (nephrotoxic), while shown to be toxic to the liver (hepatotoxic). All of the compounds tested showed high acute oral toxicity and at the same time toxic to the mitochondrial.

CONCLUSION

BMHCa and its derivatives were optimized using DFT calculations, and the HOMO energy, LUMO energy, Band gap energy, thermodynamics properties, and other reactivity descriptors were obtained. To probe further into their anticancer activities, all the compounds were docked with a human serine/threonine-protein kinase receptor, 3FC2. BHMCd showed the lowest bang gap energy, indicating the most reactive among the compounds. Also, molecular docking showed that all the compounds have stable interaction and higher binding energy with BHMCf showing the highest binding energy (-8.469 kcal mol^{-1}). Furthermore, all the compounds satisfy the Lipinski rule and are, therefore, good therapeutic candidates. This work is purely in-silico, experimental/*in-vivo* investigation is desired to further validate the compounds in MCF breast cancer treatment. The compounds could be synthesized, tested against cancer cell lines and for further clinical investigations.

REFERENCES

[1] Cancer (n.d.)., Retrieved **2021**, from https://www.who.int/newsroom/factsheets/detail/cancer

[2] Hamed, A. R.; Abdel-Azim, N. S.; Shams, K. A.; *et al*., Targeting multidrug resistance in cancer by natural chemosensitizers. *Bull. Natl. Res. Cent.,* **2019**, *43,* 8. DOI: 10.1186/s42269-0190043-8.

[3] Iqbal, J.; Ejaz, S. A.; Khan, I.; *et al*., Exploration of quinolone and quinoline derivatives as potential anticancer agents. *DARU J. Pharm. Sci.,* **2019**, *27*, 613-626. DOI: 10.1007/s40199-019-00290-3.

[4] Barr, F. A.; Sillje, H. H.; Nigg, E. A., Polo-like kinases and the orchestration of cell division. *Nat. Rev. Mol. Cell Biol*., **2004**, *5,* 429-40. DOI: 10.1038/nrm1401.

[5] Maire, V.; Nemati, F.; Richardson, M.; Vincent-Salomon, A.; Tesson, B.; Rigaill, G., *et al.* Polo-like kinase 1: a potential therapeutic option in combination with conventional chemotherapy for the management of patients with triplenegative breast cancer. *Cancer Res*., **2013**, *73*, 813-23. DOI: 10.1158/0008-5472.CAN-12-2633.

[6] Cai, X. P.; Chen, L. D.; Song, H. B.; Zhang, C. X.; Yuan, Z. W.; Xiang, X., PLK1 promotes epithelial mesenchymal transition and metastasis of gastric carcinoma cells. *Am. J. Transl. Res.,* **2016**, *8*, 4172-83.

[7] Yamada, S.; Ohira, M.; Horie, H.; Ando, K.; Takayasu, H.; Suzuki, Y., *et al.* Expression profiling and differential screening between hepatoblastomas and the corresponding normal livers: Identification of high expression of the PLK1 oncogene as a poor-prognostic indicator of hepatoblastomas. *Oncogene.,* **2004**, *23*, 5901-11. DOI: 10.1038/sj.onc.1207782

[8] Abu Almaaty, A. H.; Elgrahy, N. A.; Fayad, E.; Abu Ali, O. A.; Mahdy, A.; Barakat, L.; El Behery, M., Design, Synthesis and Anticancer Evaluation of Substituted Cinnamic Acid Bearing 2Quinolone Hybrid Derivatives. *Molecule.*, **2021**, *26*, 4724. DOI: 10.3390/molecules26164724.

[9] Zhan, X.; Qin, W.; Wang. S.; Zhao, K.; Xin, Y.; Wang, Y.; Qi, Q.; Mao, Z., Synthesis and Anticancer Activity of 3-substituted Benzoyl-4-substituted Phenyl-1H-pyrrole Derivatives. *Anticancer Agents Med. Chem*., **2017**, *17*, 821-831. DOI: 10.2174/1871520616666160923092718.

[10] Alghamdi, S. S.; Suliman, R. S.; Almutairi, K.; Kahtani, K.; Aljatli, D., Imidazole as a Promising Medicinal Scaffold: Current Status and Future Direction. *Drug Des. Devel. Ther*., **2021**, *15,* 3289-3312. DOI: 10.2147/DDDT.S307113.

[11] Goud, N. S.; Kumar, P.; Bharath, R. D., Recent Developments of Target-Based Benzimidazole Derivatives as Potential Anticancer Agents. In B. P. Nandeshwarappa, & S. S. O. (Eds.), Heterocycles - Synthesis and Biological Activities. *IntechOpen*., **2020**. DOI: https://doi.org/10.5772/intechopen.90758.

[12] Vitaku, E.; Smith, D. T.; Njardarson, J. T., Analysis of the structural diversity, substitution patterns, and frequency of nitrogen Heterocycles among U.S. FDA

approved pharmaceuticals: Mini perspective. *J. Med. Chem*., **2014**, *57*, 10257-10274

[13] Xiang, P.; Zhou, T.; Wang, L.; Sun, C.; Hu, J.; Zhao, Y.; Yang, L., Novel benzothiazole, benzimidazole and benzoxazole derivatives as potential antitumor agents: Synthesis and preliminary *in vitro* biological evaluation. *Molecules.,* **2012**, *17*, 873-883. DOI: 10.3390/molecules17010873.

[14] Marinescu, M.; Tudorache, D. G.; Marton, G. I.; Zalaru, C. M.; Popa, M.; Chifiriuc, M. C.; Stavarache, C. E.; Constantinescu, C., Density functional theory molecular modeling, chemical synthesis, and antimicrobial behaviour of selected benzimidazolederivatives. *J. Mol. Struct*., **2017**, *1130*, 463-47. DOI: 10.1016/j.molstruc.2016.10.066.

[15] Márquez-Navarro, A.; Nogueda-Torres, B.; Hernández-Campos, A.; Soria-Arteche, O.; Castillo, R.; Rodríguez-Morales, S.; Yépez-Mulia, L.; Hernández-Luis, F., Anthelmintic activity of benzimidazole derivatives against Toxocara canis second-stagelarvae and Hymenolepis nana adults. *Acta Trop*., **2009**, *109*, 232-235. DOI: 10.1016/j.actatropica.2008.11.014.

[16] Kamanna, K., Synthesis and pharmacological profile of Benzimidazoles. In: Marinescu M,, editor. Chemistry and Applications of Benzimidazole and its Derivatives. *IntechOpen*, **2019**.

[17] Song, B.; Park, E. Y.; Kim, K. J.; Ki, S. H., Repurposing of Benzimidazole Anthelmintic Drugs as Cancer Therapeutics. *Cancers*, **2022**, *14*, 4601. DOI: https://doi.org/10.3390/cancers14194601

[18] Matsa, R.; Makam, P.; Kaushik, M.; Hoti, S. L.; Kannan, T., Thiosemicarbazone derivatives: Design, synthesis and in vitro antimalarial activity studies. *Eur. J. Pharm. Sci*., **2019**, *137*, 104986. DOI: 10.1016/ j.ejps.2019.104986.

[19] Hu, W. X.; Zhou, W.; Xia, C. N.; Wen, X., Synthesis and anticancer activity of Thiosemicarbazone. *Bioorg. Med. Chem. Lett*., **2006**, *16*, 2213-2218. DOI: 10.1016/j.bmcl.2006.01.048.

[20] Oliveira, J.; Nonato, F.; Zafred, R.; Leite, N.; Ruiz, A.; Carvalho, J.; Silva, A.; Moura, R.; Lim, M., Evaluation of anti-inflammatory effect of derivative (E)-N-(4-bromophenyl)-2-(thiophen-2-ylmethylene)-thiosemicarbazone. *Biomed. Pharmacother*., **2016**, *80,* 388-392. DOI: 10.1016/j.biopha.2016.03.047.

[21] Ishaq, M.; Taslimi, P.; Shafiq, Z.; Khan, S.; Salmas, R. E.; Zangeneh, M. M.; Saeed, A.; Zangeneh, A.; Sadeghian, N.; Asari, A.; *et al*., Synthesis, bioactivity and binding energy calculations of novel 3-ethoxysalicylaldehyde based thiosemicarbazone derivatives. *Bioorg. Chem*., **2020**, *100*, 103924. https://doi.org/10.1016/j.bioorg.2020.103924.

[22] Kshirsagar, A.; Toraskar, M. P.; Kulkarni, V. M.; Dhanashire, S.; Kadam, V., Microwave assisted synthesis of potential anti-infective and anticonvulsant thiosemicarbazones. *Int. J. Chem. Tech*., **2009**, *1*, 696-701.

[23] Balogun, T. A.; Ipinloju, N.; Abdullateef, O. T.; Moses, S. I.; Omoboyowa, D. A.; James, A. C.; Saibu, O. A.; Akinyemi, W. F.; Oni, E. A., Computational Evaluation of Bioactive Compounds from Colocasia affinis Schott as Novel EGFR inhibitor for Cancer Treatment. *Cancer Inform*., **2021**, *20*, 1-12. DOI: 10.1177/ 11769351211049244.

[24] Oyeneyin, O.; Abayomi, T.; Ipinloju, N.; Agbaffa, E.; Akerele, D.; Arobadade, O., Investigation of Amino Chalcone Derivatives as Anti-Proliferative Agents against MCF-7 Breast Cancer Cell Lines-DFT, Molecular Docking and Pharmacokinetics Studies. *Adv. J. Chem. A*., **2021**, *4*, 288-299. DOI: 10.22034/ ajca.2021.285869.1261.

[25] Surabhi, S.; Singh, B. K., Computer aided drug design: an overview. *J. Drug Deliv. and Ther.,* **2018**, *8*, 504-9. DOI: 10.22270/jddt.v8i5.1894.

[26] Ramalingam, A., Hirshfeld surface analysis, interaction energy calculation and spectroscopical study of 3-chloro-3-methyl-r(2),(6)-bis(p-tolyl)piperidin-4-one using DFT approaches, *J. Mol. Struct*., ***2022***, *1248*,131483. DOI: 10.1016/j.molstruc.2021.131483.

[27] Ramalingam, A.; Mustafa, N.; Chng, W. J.; Medimagh, M.; Sambandam, S.; Issaoui, N., 3-Chloro-3-methyl-2,6-diarylpiperidin-4-ones as Anti-Cancer Agents: Synthesis, Biological Evaluation, Molecular Docking, and *In Silico* ADMET Prediction. *Biomolecules.,* **2022**, *12*, 1093. DOI: 10.3390/ biom12081093.

[28] Ojo, N. D.; Krause, R. W.; Obi-Egbedi, N. O., Electronic and nonlinear optical properties of 3-(((2-

substituted-4-nitrophenyl)imino) methyl)phenol. *Comput. Theor. Chem.,* **2020**, *1192*, 1-8. DOI: 10.1016/ j.comptc.2020.113050.

[29] Kumar, A.; Sambandam, S.; Ramalingam, A.; Krishnamoorthy, R.; Arumugam, D.; Oyeneyin, O. E., Synthesis, molecular docking of 3-(2-chloroethyl)-2,6-diphenylpiperidin-4-one: Hirshfeld surface, spectroscopic and DFT based analyses. *Journal of Molecular Structure* **2022**, *1262*, 132993. https://doi.org/10.1016/j.molstruc.2022.132993.

[30] Arulraj, R.; Sivakumar, S.; Suresh, S.; Anitha, K., Synthesis, vibrational spectra, DFT calculations, Hirshfeld surface analysis and molecular docking study of 3-chloro-3-methyl-2,6-diphenylpiperidin-4-One. *Spectrochim, Acta A. Mol. Biomol. Spectrosc*, **2020**, *232,* 118166. https://doi.org/10.1016/j.saa.2020.118166.

[31] Ramalingam, A.; Guerroudj, A. R.; Sambandam, S.; Kumar, A.; Krishnamoorthy, R.; Boukabcha, N.; Chouaih, A.; Elayaperumal, M., Synthesis, vibrational spectra, Hirshfeld surface analysis, DFT calculations, and in silico ADMET study of 3-(2-chloroethyl)-2,6-bis(4-fluorophenyl)piperidin-4 one: A potent anti-Alzheimer agent, *J. Mol. Struct*., **2022**, *1269*, 133845. https://doi.org/10.1016/j.molstruc.2022.133845.

[32] Ramalingam, A.; Sivakumar, S.; Mouna, M.; Omar, A. L.; Noureddine, I.; Marek, J. W., Study of a new piperidone as an anti-Alzheimer agent: Molecular docking, electronic and intermolecular interaction investigations by DFT method. *J. King Saud. Univ. Sci*., **2021**, *33*, 101632. DOI: 10.1016/j.jksus.2021.101632.

[33] Eniafe, G. O.; Metibemu, D. S.; Omotuyi, O. I.; Ogunleye, A. J.; Inyang, O. K.; Adelakun, N. S.; Adeniran, Y. O.; Adewumi, B.; Enejoh, O. A.; Osunmuyiwa, J. O.; Shodehinde, S. A.; Oyeneyin, O. E., Agemone mexicana flavanones; apposite inverse agonists of the β2-adrenergic receptor in asthma treatment. *Bioinform*. **2018**, *14*, 60-67. DOI: 10.6026/ 97320630014060.

[34] Ubeid, M. T.; Thabet, H. K.; Abu Shuheil, M. Y., Synthesis of 4-[(1H-Benzimidazol-2yl)sulfanyl] benzaldehyde and 2-({4-[(1H-Benzimidazol-2-yl)sulfanyl]phenyl}methylidene) hydrazine-1-carbo-thioamide. *Molbank*., **2021**, *2021*, M1273. DOI: 10.3390/M1273.

[35] Ipinloju, N.; Ibrahim, A.; da Costa, R. A.; Adigun, T. B.; Olubode, S. O.; Abayomi, K. J.; Aiyelabegan, A. O.; Esan, T. O.; Alhaji Muhammad, S.; Oyeneyin O. E., Quantum Evaluation and Therapeutic Activity of (E)-N-(4-methoxyphenyl)-2-(4-(3-oxo-3-phenylprop-1-en-1-yl) phenoxy)acetamide and its Modified Derivatives against EGFR and VEGFR-2 in the Treatment of Triple Negative Cancer via *In Silico* Approach. *J. Mol. Model.,* **2023**, *29,* 159. DOI: 10.1007/s00894-023-05543-2.

[36] Oyeneyin, O. E.; Ojo, N. D.; Ipinloju, N.; James, A. C.; Agbaffa, E. B., Investigation of Corrosion Inhibition Potentials of Some Aminopyridine Schiff Bases Using Density Functional Theory and Monte Carlo Simulation. *Chem. Africa*., **2022**, *5*, 319-332. DOI: 10.1007/s42250-02100304-1.

[37] Shao, Y.; Molnar L. F.; Jung Y. *et al*., SPARTAN '14, build 1.01. Irvine (CA): Wavefunction Inc., **2014**.

[38] Becke, A. D., Density-functional thermochemistry. III. The role of exact exchange. *J. Chem. Phys*., **1993**, *98*, 5648-5652. DOI: 10.1063/1.464913.

[39] Jensen, F., Polarization consistent basis sets: principles. *J. Chem. Phys*., **2001**, *115*, 9113-9125. DOI: 10.1063/ 1.1413524.

[40] Hazhazi, H.; Melkemi, N.; Bouachrine, M., DFT-based reactivity and combined QSAR, molecular docking of 1,2,4,5-Tetrazine derivatives as inhibitors of Pim-1 kinase. *Heliyon*., **2019**, *5*, 0-9. DOI: 10.1016/ j.heliyon.2019.e02451.

[41] Ramalingam, A.; Kansız, S.; Dege, N. *et al.* Synthesis, Crystal Structure, DFT Calculations and Hirshfeld Surface Analysis of 3-Chloro-2,6-Bis(4-Chlorophenyl)-3-Methylpiperidin-4-One. *J. Chem. Crystallogr*., **2021**, *51*, 273-287. https://doi.org/10.1007/s10870-020-00852-3.

[42] Geerlings, P.; De, Proft F., Chemical Reactivity as Described by Quantum Chemical Methods. *Int. J. Mol. Sci*., **2002**, *3*, 276-309. DOI: 10.3390/i3040276.

[43] Koopmans, T., Ordering of wave functions and eigenenergies to the individual electrons of an atom. *Physica.,* **1933**, *1*, 104-113. DOI:10.1016/S0031-8914(34)90011-2.

[44] Parr, R. G.; Pearson, R. G., Absolute Hardness: Companion Parameter to Absolute Electronegativity.

J. Am. Chem. Soc., **1983**, 7512-7516. DOI: 10.1021/ ja00364a005.

[45] Maestro. **2018**, Maestro. Schrödinger, LLC.

[46] Ramalingam, A.; Kuppusamy, M.; Sambandam, S.; Medimagh, M.; Oyeneyin, O. E.; Shanmugasundaram, A.; Issaoui, N.; Ojo, N. D., Synthesis, spectroscopic, topological, hirshfeld surface analysis, and anti-covid-19 molecular docking investigation of isopropyl 1-benzoyl-4-(benzoyloxy)-2,6-diphenyl-1,2,5,6-tetra-hydropyridine-3-carboxylate. *Heliyon* **2022**, *8* (10), e10831.

[47] LigPrep. **2018**. LigPrep. Schrödinger, LLC.

[48] Friesner, R. A.; Banks, J. L.; Murphy, R. B.; Halgren, T. A.; Klicic, J. J.; Mainz, D. T.; Repasky, M. P.; Knoll, E. H.; Shelley, M.; Perry, J. K.; Shaw, D. E.; Francis, P.; Shenkin, P. S., Glide: A new approach for rapid, accurate docking and scoring. 1. Method and assessment of docking accuracy. *J. Med. Chem*., **2004**, *47*, 1739-1749. DOI: 10.1021/jm0306430.

[49] Aziz, M.; Ejaz, S. A.; Tamam, N. *et al.* Identification of potent inhibitors of NEK7 protein using acomprehensive computational approach. *Sci Rep.,* **2022**, *12*, 6404. DOI:10.1038/s41598-022.

[50] Saeed, A.; Ejaz, S. A.; Sarfraz, M.; Tamam, N.; Siddique, F.; Riaz, N.; Qais, F. A.; Chtita, S.; Iqbal, J., Discovery of Phenylcarbamoylazinane-1,2,4-Triazole Amides Derivatives as the Potential Inhibitors of Aldo-Keto Reductases (AKR1B1 & AKRB10): Potential Lead Molecules for Treatment of Colon Cancer. *Molecules.,* **2022**, *27*, 3981. DOI: 10.3390/ molecules27133981.

[51] Prime. **2019**. Prime. Schrödinger, LLC.

[52] Genheden, S.; Ryde, U., The MM/PBSA and MM/GBSA methods to estimate ligand-binding affinities. *Expert. Opin. Drug Discov.,* **2015**, *10*, 449-461. DOI: 10.1517/17460441.2015.1032936.

[53] Cheng, F.; Li W, Zhou Y.; *et al*., ADMET-SAR: a comprehensive source and free tool for asessment of chemical ADMET properties. *J. Chem. Inf. Model*., **2012**, *52*, 3105. DOI: 10.1021/ci300367a.

[54] Al-Makhzumi, Q. M. A. H.; Abdullah, H. I.; AL-Ani, R. R., Theoretical study of N-Methyl3-phenyl-3-(-4-(Trifluoromethyl)phenoxy)propan as a Drug and its Five Derivatives. *J. Biosci. Med*., **2018**, *6,* 80-98. DOI: 10.4236/jbm.2018.68007.

[55] Obot, I. B.; Kaya, S.; Kaya, C.; Tüzün, B., Theoretical evaluation of triazine derivatives as steel corrosion inhibitors: DFT and Monte Carlo simulation approaches. *Res. Chem. Intermed*., **2016**, *42*, 4963-4983. DOI: 10.1007/s11164-015-2339-0.

[56] Garbett, N. C.; Chaires, J. B., Thermodynamic studies for drug design and screening. *Expert Opin. Drug Discov*., **2012**, *7*, 299-31. DOI: 10.1517/ 17460441.2012.666235.

[57] Ossama, D.; Souad, E.; Chtita, S., Design and Prediction of ADME/Tox Properties of Novel Magnolol Derivatives as Anticancer Agents for NSCLC Using 3D-QSAR, Molecular Docking, MOLCAD and MM-GBSA Studies. *Lett. Drug Des. Discov*., **2022**, *19*. DOI: 10.2174/1570180819666220510141710.

[58] Fouedjou, R.T.; Chtita, S.; Bakhouch, M.; Belaidi, S., Ouassaf, M.; Djoumbissie L. A.; Tapondjou, L. A.; Qais, F. A., Cameroonian medicinal plants as potential candidates of SARS-CoV-2 inhibitors. *J. Biomol. Struct. Dyn*., **2021**. DOI: 10.1080/ 07391102.2021.1914170.

[59] Strebhardt, K., Multifaceted polo-like kinases: drug targets and antitargets for cancer therapy. *Nat Rev Drug Discov*., **2010**, *9*, 643-660. DOI: 10.1038/nrd3184.

[60] Grinshtein, N.; Datti, A.; Fujitani, M.; Uehling, D.; Prakesch, M.; Isaac, M.; Irwin, M. S.; Wrana, J. L.; Al-Awar, R.; Kaplan, D. R., Small molecule kinase inhibitor screen identifies polo-like kinase 1 as a target for neuroblastoma tumorinitiating cells. *Cancer Res.,* **2011**, *71*, 1385-1395.

[61] Oyeneyin, O. E.; Iwegbulam, C. G.; Ipinloju, N.; Olajide, B. F.; Oyebamiji, A. K., Prediction of the antiproliferative effects of some benzimidazole-chalcone derivatives against MCF-7 breast cancer cell lines: QSAR and molecular docking studies. *Org. Commun.*, **2022**, 273-287. DOI: http://doi.org/10.25135/acg.oc.132.2203.2374.

[62] Tahlan, S.; Kumar, S.; Ramasamy, K., *et al. In-silico* molecular design of heterocyclic benzimidazole scaffolds as prospective anticancer agents. *BMC Chem.*, **2019**, *13*, 90. DOI: https://doi.org/10.1186/s13065-019-0608-5.

[63] Ibrahim, A.; Ipinloju, N.; Aiyelabegan, A O.; Alfa-

Ibrahim, A. A.; Muhammad, S. A.; Oyeneyin, O. E., Discovery of Potential Phytochemicals from Carica papaya Targeting BRCA-1 in Breast Cancer Treatment. Applied Biochemistry and Biotechnology. **2023** Mar 29, 1-7.

[64] Wanat, K., Biological barriers, and the influence of protein binding on the passage of drug across them. *Mol. Biol. Rep.,* **2020**, *47*, 3221-3231. DOI: 10.1007/s11033-020-05361-2.

[65] Smith, D.; Di, L.; Kerns, E., The effect of plasma protein binding on in vivo efficacy: misconceptions in drug discovery. *Nat. Rev. Drug Discov*., **2010**, *9*, 929-39. DOI: 10.1038/nrd3287.

[66] Song, Y.; Li, C.; Liu, G.; Liu, R.; Chen, Y.; Li, W.; *et al*., Drug-Metabolizing Cytochrome P450 Enzymes Have Multifarious Influences on Treatment Outcomes. *Clin. Pharmacokinet*., **2021**, *60*, 585-601. DOI: 10.1007/s40262-021-01001-5.

[67] Kazmi, S. R.; Jun, R.; Yu, M. S.; Jung, C.; Na, D., *In silico* approaches and tools for the prediction of drug metabolism and fate: A review. *Comput. Biol. Med*., **2019**, *106*, 54-64. DOI: 10.1016/ j.compbiomed.2019.01.008.

[68] Zhang, Z.; Tang, W., Drug metabolism in drug discovery and development. *Acta Pharm. Sin. B*. **2018***,* *8*, 721-32. DOI: 10.1016/j.apsb.2018.04.003.

[69] Fatunde, O. A.; Brown, S. A., The Role of CYP450 Drug Metabolism in Precision Cardio-Oncology. *Int. J. Mol. Sci*., **2020**, *21*, 604. DOI: 10.3390/ijms21020604.

[70] Jia, C. Y.; Li, J. Y.; Hao, G. F.; Yang, G. F., A drug-likeness toolbox facilitates ADMET study in drug discovery. *Drug Discov. Today*., **2020**, *25*, 248-58. DOI: 10.1016/j.drudis.2019.10.014.

.